Modelling the excavation damaged zone in claystone with strain localisation using coupled second gradient model and the influence of gallery ventilation

B. Pardoen - S. Levasseur - F. Collin

Université de Liège – ArGEnCo

Beinjing, China, Septembre 8, 2014

Outline

1. FRACTURING EVIDENCES

2. MATERIAL BEHAVIOUR

3. NUMERICAL RESULTS FOR GALLERY EXCAVATION

4. CONCLUSIONS AND OUTLOOKS

Outline

1. **FRACTURING EVIDENCES**
2. MATERIAL BEHAVIOUR
3. NUMERICAL RESULTS FOR GALLERY EXCAVATION
4. CONCLUSIONS AND OUTLOOKS

1. Fracturing evidences

Mechanical fracturing :

Small scale (laboratory) :

- Loading
- Strain localization in shear band mode
- Rupture

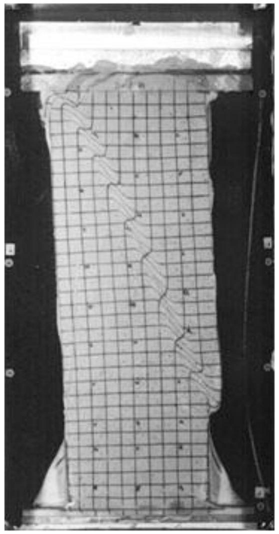

Mokni and Desrues,1999

Large scale (galleries) :

- Excavation
- Stress redistribution
- Fracturing / Damage zone

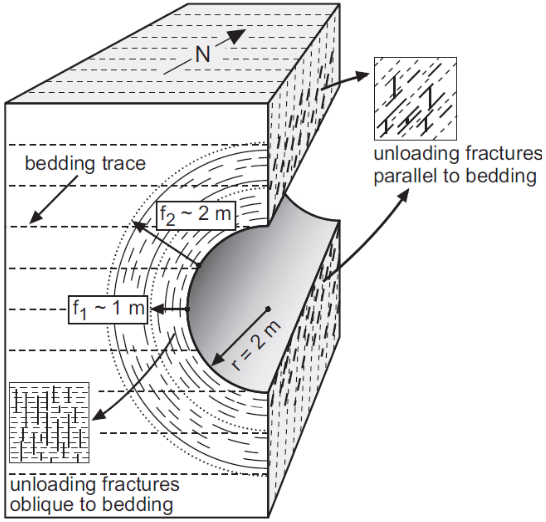

Bossart et al., 2002

In situ evidences :

Observations and measurements (ANDRA URL, GED Gallery, Cruchaudet *et al.* 2010a).

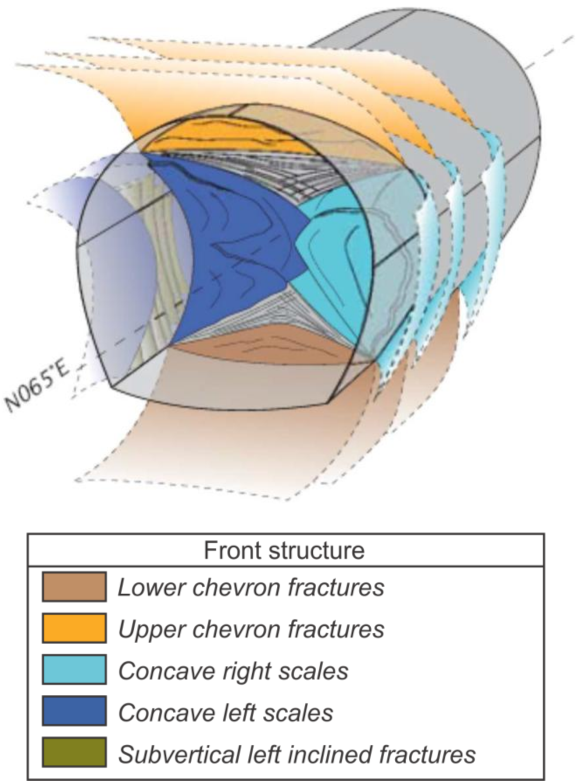

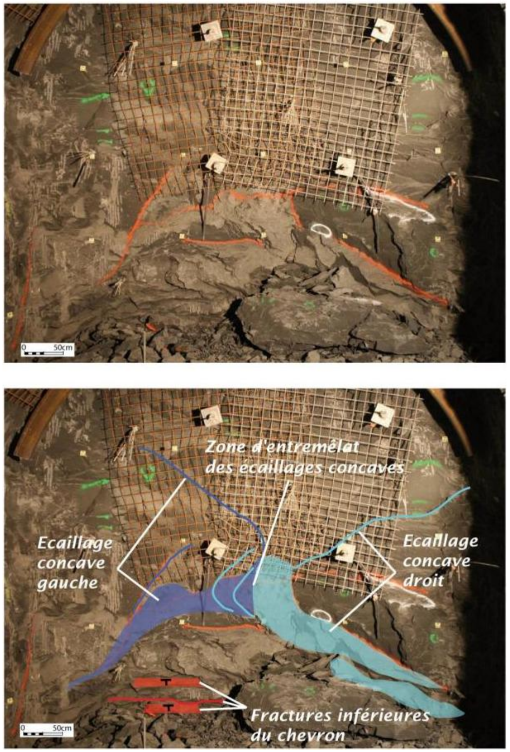

Front of the section GED1002

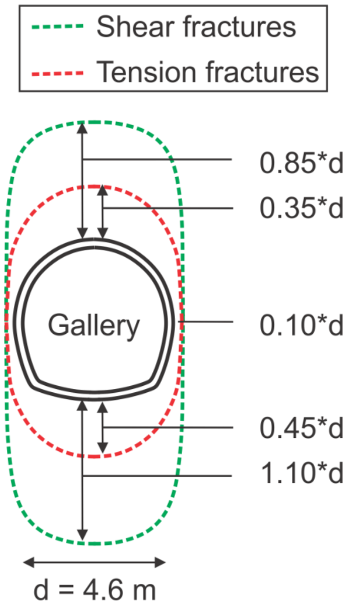

Major issues : prediction of the extension and fracturing structure.

study
- damaged zone development with shear strain localisation,
- influence of the gallery ventilation.

Outline

1. FRACTURING EVIDENCES

2. **MATERIAL BEHAVIOUR**

3. NUMERICAL RESULTS FOR GALLERY EXCAVATION

4. CONCLUSIONS AND OUTLOOKS

Material :

Partially saturated porous media, 2 phases : solid + water

Homogenised mixture mass density : $\rho = \rho_s (1-n) + \rho_w \, n \, S_{r,w}$

Bishop's stress definition : $\sigma_{ij} = \sigma'_{ij} - b \, S_{r,w} \, p_w \, \delta_{ij}$

Solid phase behaviour :

Solid grain density variation : $\dfrac{\partial \rho_s}{\partial t} = \dfrac{\rho_s}{K_s}\left[(b-n) S_{r,w} \dfrac{\partial p_w}{\partial t} - \dfrac{\partial \sigma'}{\partial t}\right]$

Biot's coefficient : $b = 1 - \dfrac{K_0}{K_s}$

Porosity variation: $\dfrac{\partial n}{\partial t} = (1-n)\left[\dfrac{1}{\rho_s}\dfrac{\partial \rho_s}{\partial t} + \dfrac{\partial \varepsilon_v}{\partial t}\right]$

Fluid phase behaviour :

Fluid mass flow (advection, Darcy) : $m_{w,i} = -\rho_w \dfrac{k \, k_{r,w}}{\mu_w}\left(\dfrac{\partial p_w}{\partial x_i} + \rho_w g_i\right)$

Water retention and permeability curves (Van Genuchten's model) : $S_{r,w} = \left[1 + \left(\dfrac{p_c}{P_r}\right)^N\right]^{-M}$ $\quad k_{r,w} = \sqrt{S_{r,w}}\left[1 - \left(1 - S_{r,w}^{1/M}\right)^M\right]^2$

Mechanical model – 1st gradient model :

The constitutive mechanical law for the clayey rock is :

- a non-associated elasto-plastic internal friction model, with a Drucker-Prager yield surface

$$F \equiv II_{\hat{\sigma}} - m\left(I_{\sigma} + \frac{3c}{\tan\phi_C}\right) = 0$$

$$I_{\sigma} = \sigma_{ij}\delta_{ij} \qquad II_{\hat{\sigma}} = \sqrt{\frac{1}{2}\hat{\sigma}_{ij}\hat{\sigma}_{ij}} \qquad m = \frac{2\sin\phi_c}{\sqrt{3}\left(3-\sin\phi_c\right)}$$

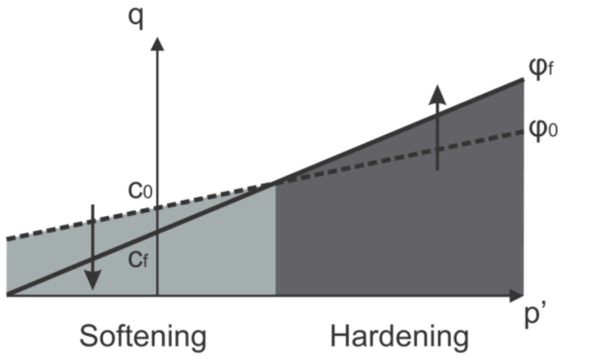

- allowing hardening/softening of φ and/or c as a function of the Von Mises equivalent plastic strain ε^p_{eq}

$$\varepsilon^p_{eq} = \sqrt{\frac{2}{3}\hat{\varepsilon}^p_{ij}\hat{\varepsilon}^p_{ij}}$$

$$\phi_C = \phi_{C0} + \frac{\left(\phi_{Cf} - \phi_{C0}\right)\varepsilon^p_{eq}}{B_\phi + \varepsilon^p_{eq}}$$

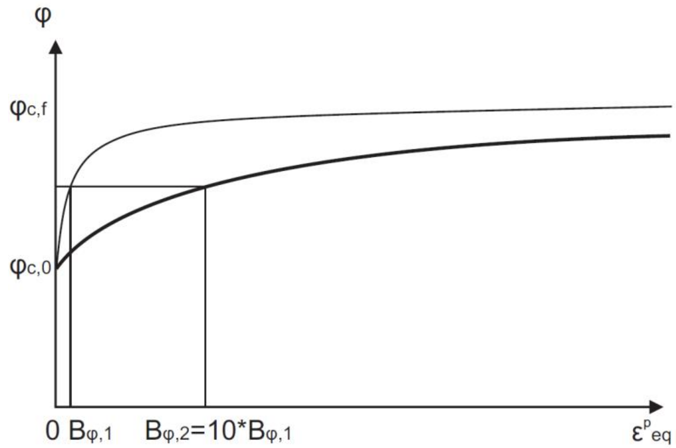

<u>Modelling of strain localisation – 2^d gradient model :</u> (Chambon *et al.*, 1998 and 2001)

The continuum is enriched with <u>microstructure effects</u>. The kinematics include the classical one (macro) and the microkinematics (Toupin 1962, Mindlin 1964, Germain 1973, Collin et al., 2006).

Balance equations :

$$\int_{\Omega}\left(\sigma_{ij}\frac{\partial u_i^*}{\partial x_j}+\Sigma_{ijk}\frac{\partial^2 u_i^*}{\partial x_j \partial x_k}\right)d\Omega=\int_{\Omega}G_i u_i^* d\Omega+\int_{\Gamma_\sigma}\left(\bar{t}_i u_i^*+\bar{T}_i D u_i^*\right)d\Gamma$$

$$\int_{\Omega}\left(\frac{\partial M}{\partial t}p_w^*-m_i\frac{\partial p_w^*}{\partial x_i}\right)d\Omega=\int_{\Omega}Q\,p_w^*\,d\Omega+\int_{\Gamma_q}\bar{q}\,p_w^*\,d\Gamma$$

Σ_{ijk} is the double stress, which need an additional constitutive law : linear elastic law (Mindlin, 1964) defined as a function of the (micro) second gradient of displacement field u_i^* :

$$\tilde{\Sigma}_{ijk}=f\left(D,\frac{\partial^2 u_i^*}{\partial x_j \partial x_k}\right)$$

It depends only on one elastic parameter D. The shear band width is proportional to this parameter. (Chambon *et al.,* 1998, Kotronis et al., 2007).

Mechanical and hydraulic parameters :

Synthesis of Callovo-Oxfordian claystone parameters from (Charlier et al. 2012)

Symbol	Name	Value	Unit
k_{hor}	Horizontal intrinsic water permeability	$4\ 10^{-20}$	m²
k_{vert}	Vertical intrinsic water permeability	$1.33\ 10^{-20}$	m²
n_0	Porosity	0.18	-
M	Van Genuchten coefficient	0.33	-
N	Van Genuchten coefficient	1.49	MPa
P_r	Van Genuchten parameter	15	Pa^{-1}

Symbol	Name	Value	Unit
E	Young's modulus	4000	MPa
ν	Poisson's ratio	0.3	-
b	Biot's coefficient	0.6	-
ρ_s	Specific mass	2300	kg/m³
ψ	Dilatancy angle	0.5	°
φ_0	Initial friction angle	10	°
φ_f	Final friction angle	20	°
B_φ	Friction angle hardening coefficient	0.002	-
c_0	Initial cohesion	3	MPa
c_f	Final cohesion	0.3	MPa
B_c	Cohesion softening coefficient	0.003	-
D	Second gradient elastic parameter	5000	N

→ Friction angle hardening

→ Cohesion softening

Outline

1. FRACTURING EVIDENCES
2. MATERIAL BEHAVIOUR
3. **NUMERICAL RESULTS FOR GALLERY EXCAVATION**
   - **2D**
   - 3D
4. CONCLUSIONS AND OUTLOOKS

Numerical modelling (LAGAMINE-ULg) :

By symmetry: quarter of the gallery

HM modelling in 2D plane strain state.
Gallery radius = 2.3 m.

Anisotropy (Andra URL) :

→ hydraulic permeability anisotropy

$k_{hor/vert} = 4\ 10^{-20}$ / $1.33\ 10^{-20}$ [m²]

→ initial anisotropic stress state

$p_{w,0} = 4.5$ [Mpa]
$\sigma_{y,0} = \sigma_{z,0} = 12$ [Mpa]
$\sigma_{x,0} = 15.6$ [MPa]

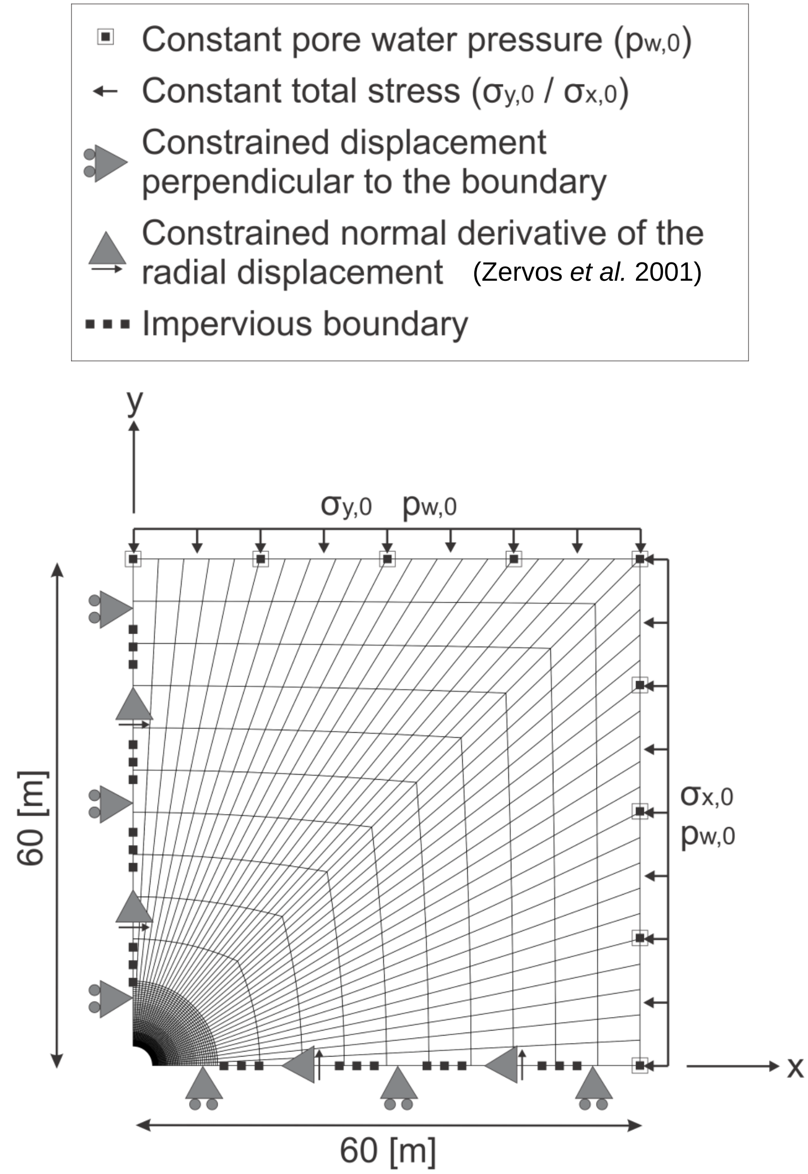

Numerical modelling (LAGAMINE-ULg) :

Pressure at gallery wall :

→ gallery excavation : σ_x and σ_y decrease

→ gallery ventilation : water phases equilibrium (Kelvin's law)

$$RH = \frac{p_v}{p_{v,0}} = exp\left(\frac{-s\,M_v}{RT\,\rho_w}\right)$$

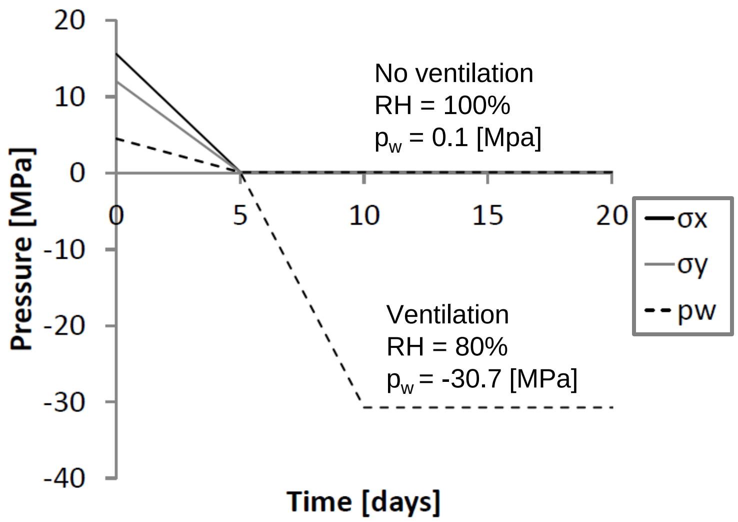

Localisation zone : no ventilation

End of excavation

↓

Total deviatoric strain

Plasticity

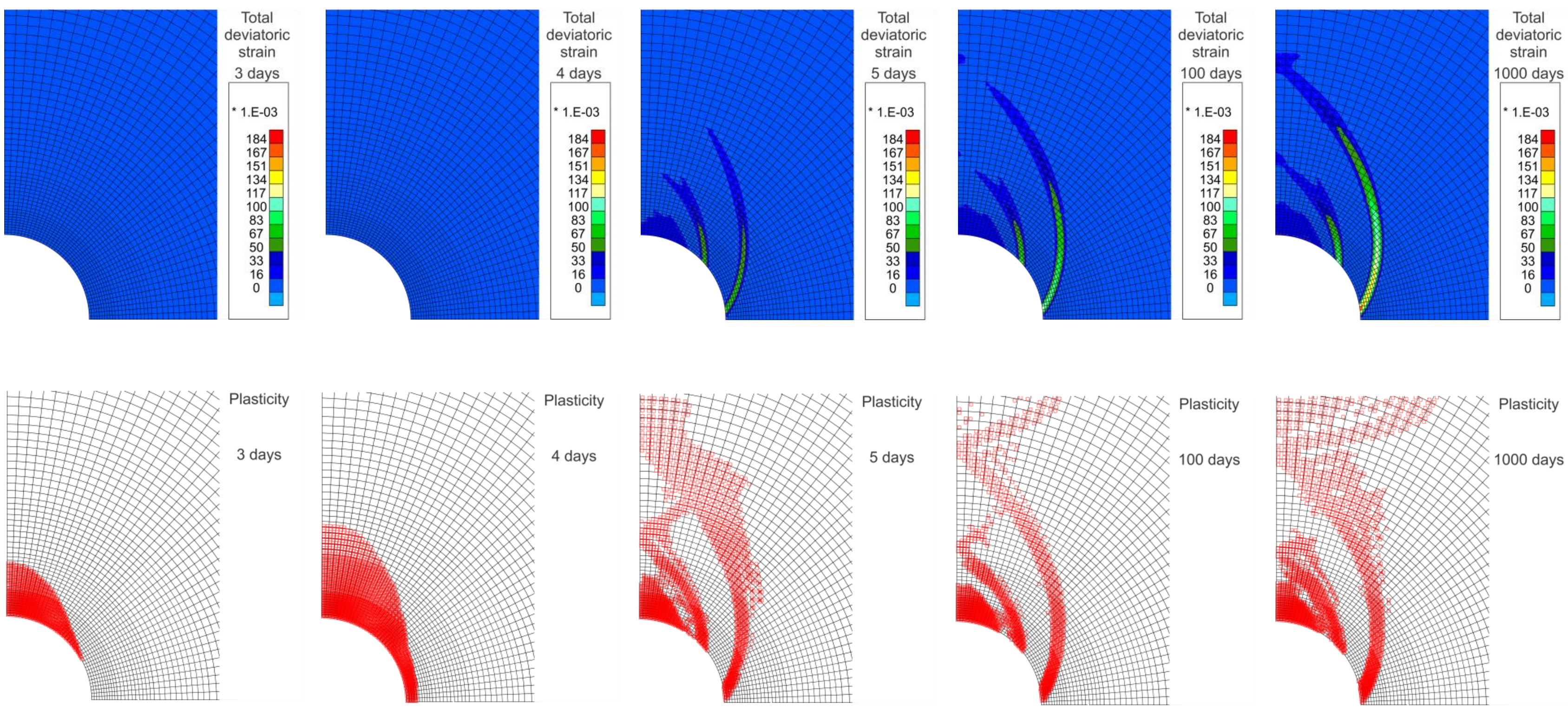

Localisation zone : ventilation

End of excavation
↓

Total deviatoric strain

Plasticity

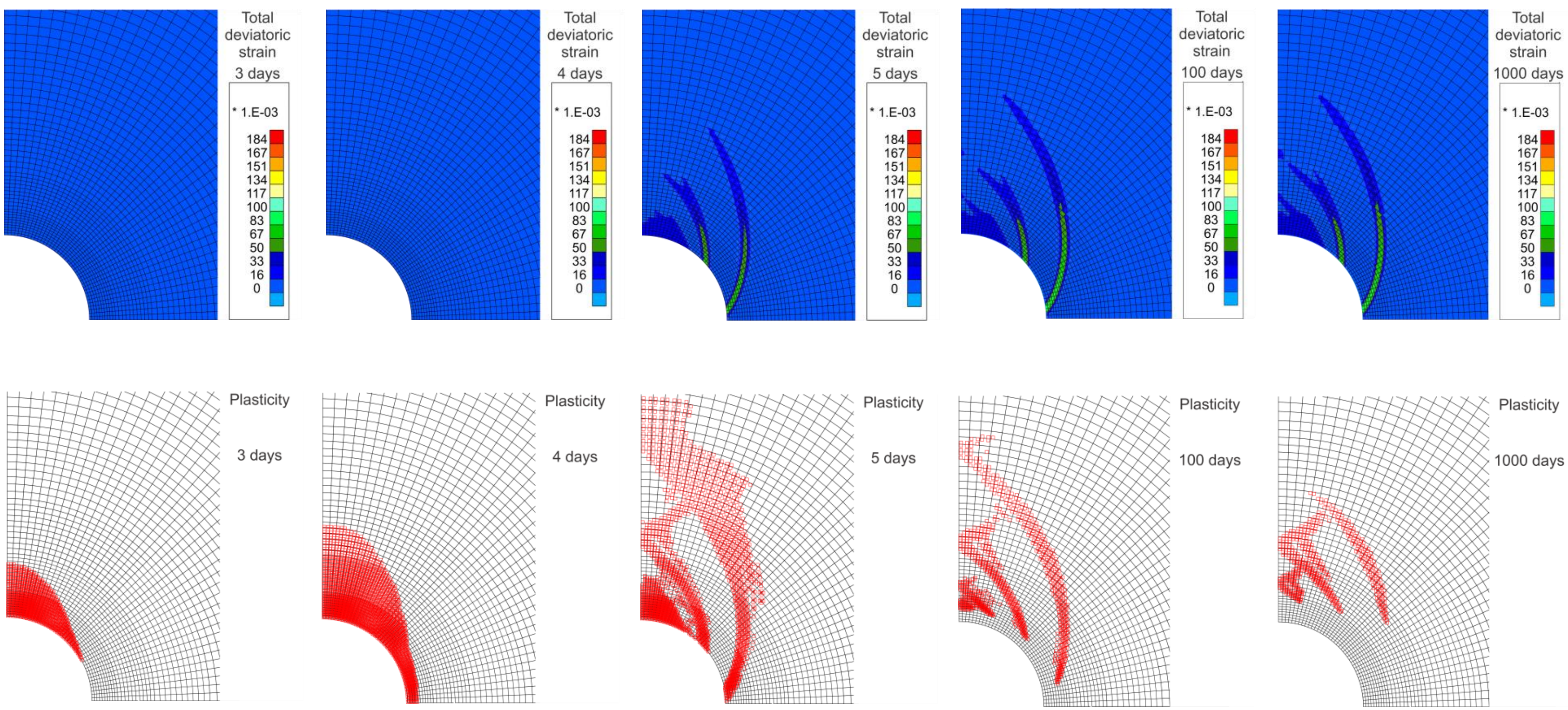

3. Numerical results for gallery excavation – 2D

Localisation zone :

Chevron fracture pattern corresponding to in situ observations (Cruchaudet *et al.*, 2010b).

Chevron fractures concentrated above the gallery because of the anisotropic stress state.

The extension of the excavation damaged zone obtained numerically corresponds fairly well to the *in situ* experimental measurements of shear fractures.

Numerical result
Shear strain localisation

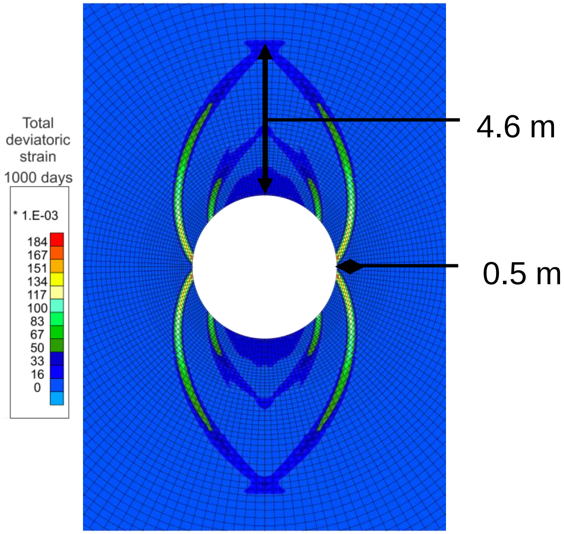

Observations
Shear fractures

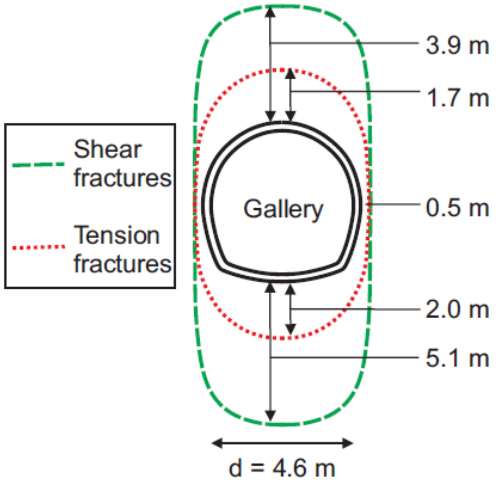

Cross sections :

Vertical

Horizontal

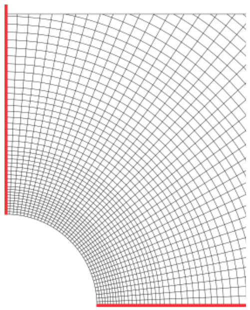

Pore water pressure

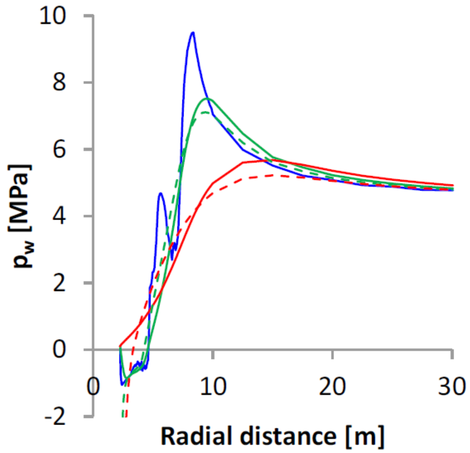

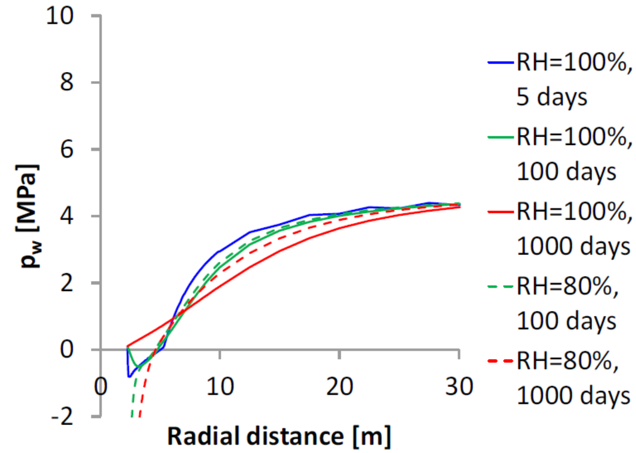

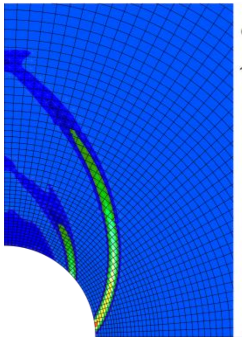

Degree of saturation

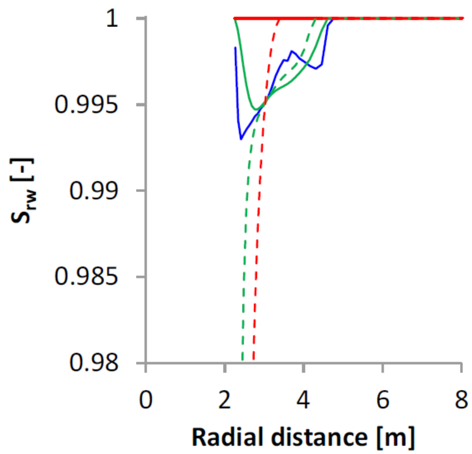

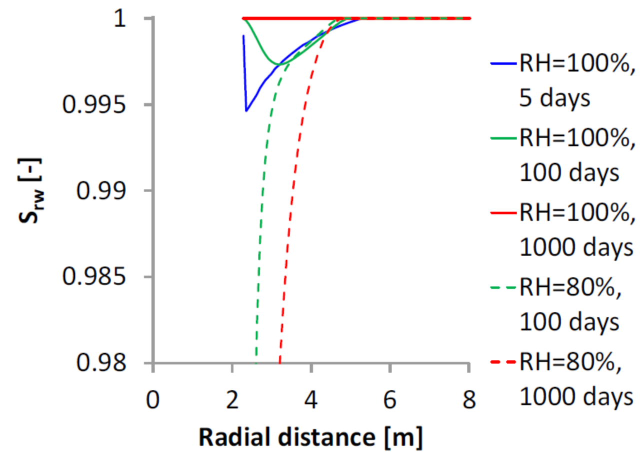

Convergence :

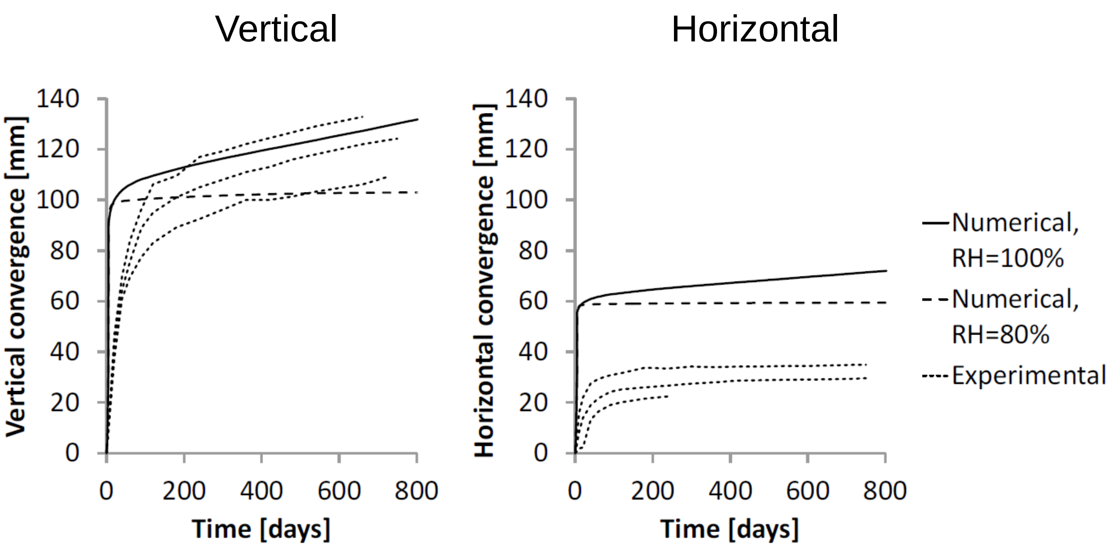

Important during the excavation and keeps increasing afterwards.

Anisotropic convergence because of the shear strain localisation bands located above the gallery.

Experimental results from a gallery of the Andra URL (Cruchaudet *et al.*, 2010b).
Good matching in the vertical direction for the modelling without ventilation.

Outline

1. FRACTURING EVIDENCES
2. MATERIAL BEHAVIOUR
3. **NUMERICAL RESULTS FOR GALLERY EXCAVATION**
   - 2D
   - **3D**
4. CONCLUSIONS AND OUTLOOKS

<u>Numerical modelling (LAGAMINE-ULg) :</u>

Mechanical modelling in 3D state.

Classical FE, no second gradient !

Initial anisotropic stress state (Andra URL) :

$\sigma_{y,0} = \sigma_{z,0} = 12$ [Mpa]

$\sigma_{x,0} = 15.6$ [MPa]

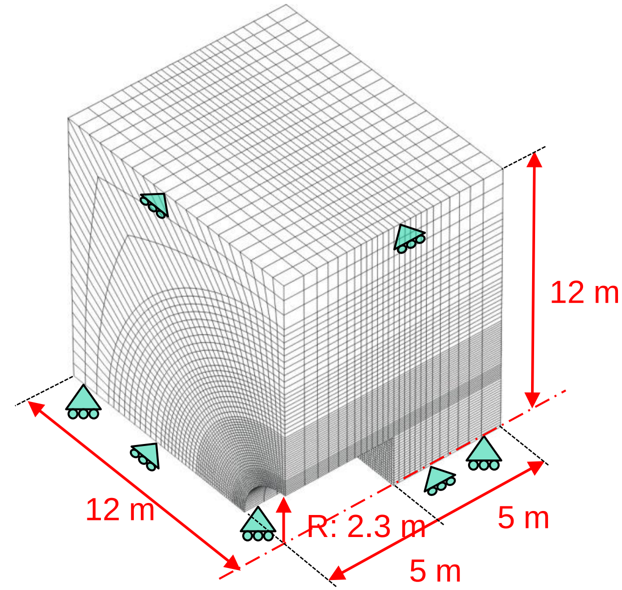

Identical excavation :

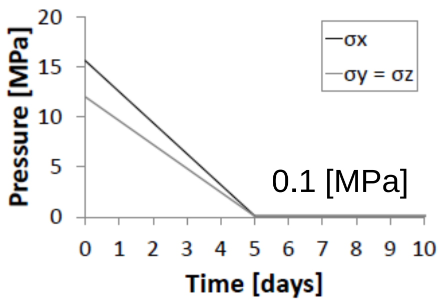

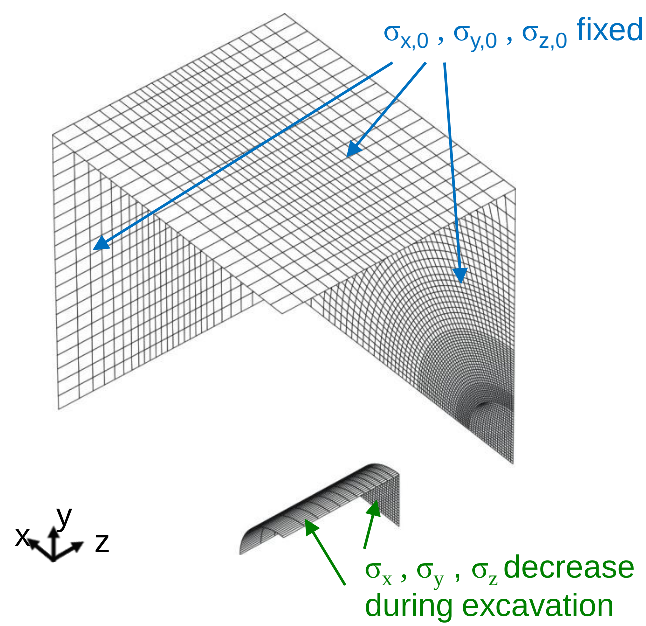

Mesh : 410 591 nodes
60 320 volume elements with 20 nodes
4 480 elements of stress imposition
752 226 equations
8 days of calculation

Equivalent deformation ε_{eq} :

ε_{eq} during boring :

3 days	3.25 days	3.5 days	3.75 days	4 days	4.25 days
$\sigma/\sigma_0 = 0.40$	$\sigma/\sigma_0 = 0.35$	$\sigma/\sigma_0 = 0.30$	$\sigma/\sigma_0 = 0.25$	$\sigma/\sigma_0 = 0.20$	$\sigma/\sigma_0 = 0.15$

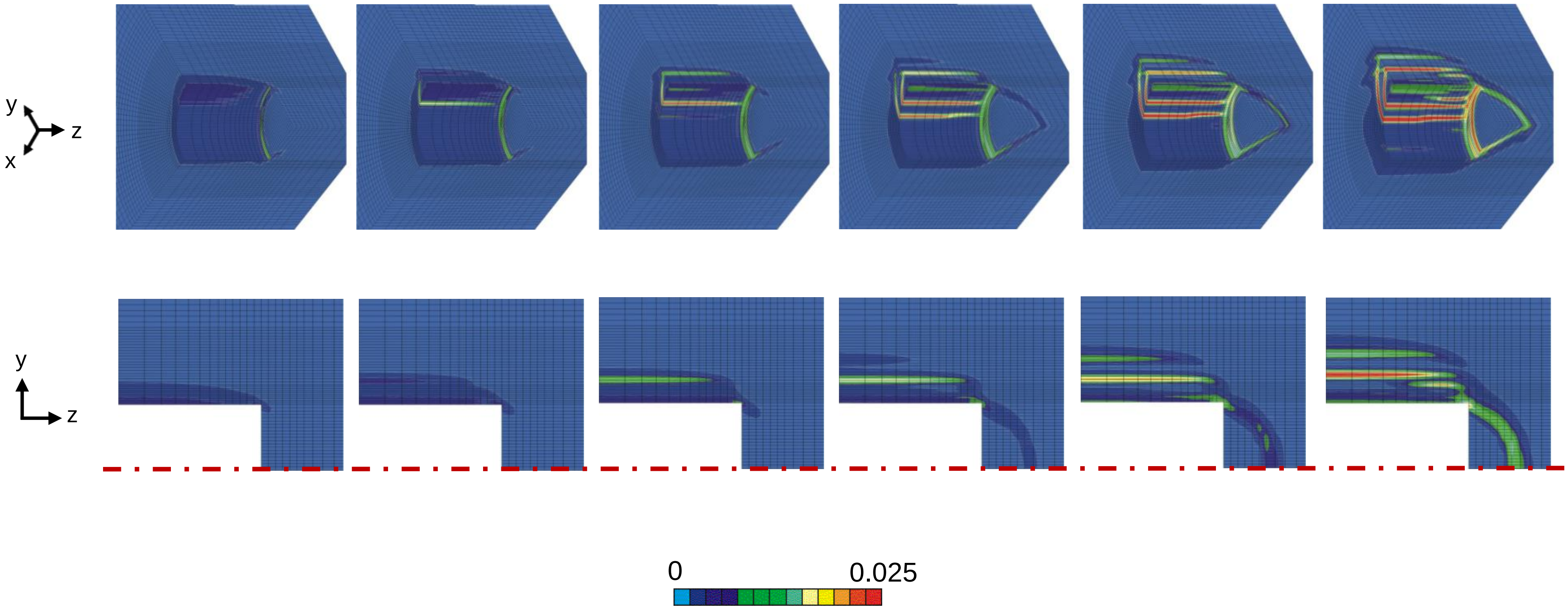

Equivalent deformation ε_{eq} :

ε_{eq} for 4.25 days of excavation ($\sigma/\sigma_0 = 0.15$) :

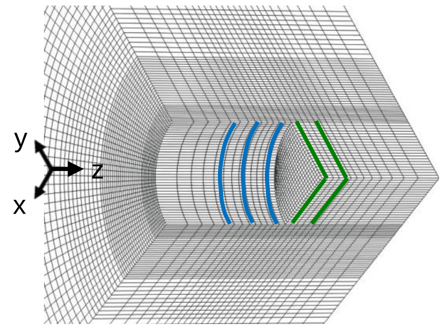

z<0 : excavation zone
z=0 : gallery end
z>0 : rock mass

z=-2.25m | z=-1.25m | z=-0.25m | z=+0.25m | z=+1.25m

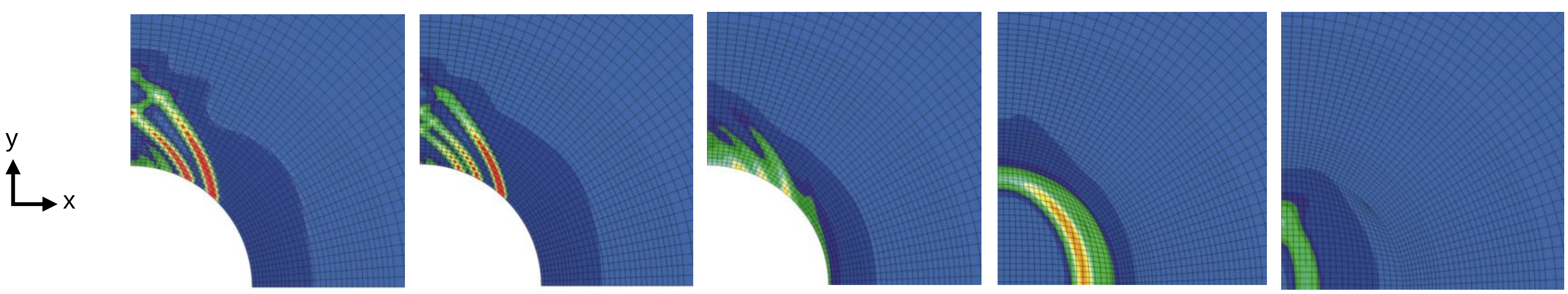

Outline

4. Conclusions and outlooks

Damaged zone → strain localisation zone similar to *in situ* measurements

→ modelling provide information about the rock structure and evolution within this zone, as observed *in situ*.

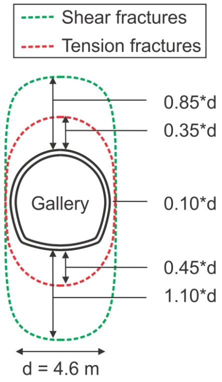

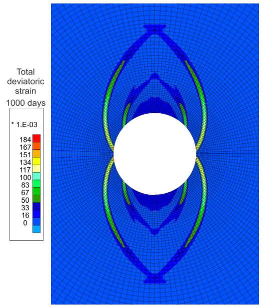

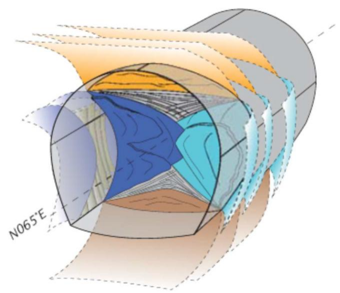

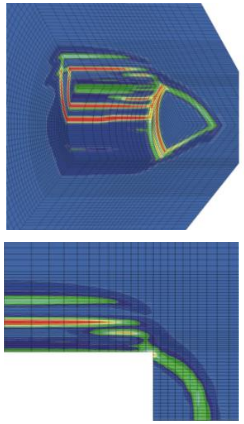

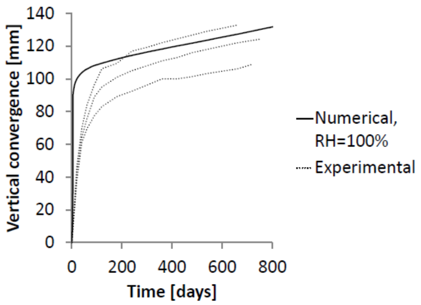

.

→ need for a <u>better definition of :</u>

<u>- the rock anisotropy</u>

<u>- the properties changes</u>

<u>- the hydromechanical coupling</u>

References

Bossart P., Meier P. M., Moeri A., Trick T., Mayor J.C., “Geological and hydraulic characterisation of the excavation disturbed zone in the Opalinus Clay of the Mont Terri Rock Laboratory”, Engineering Geology, vol. 66, n° 1-2, 2002, p. 19–38.

Chambon R., Caillerie D., El Hassan N., “One-dimensional localisation studied with a second grade model”, European Journal of Mechanics - A/Solids, vol. 17, n° 4, 1998, p. 637–656.

Chambon R., Caillerie D., Matsushima T., “Plastic continuum with microstructure, local second gradient theories for geomaterials : localization studies”, International Journal of Solids and Structures, vol. 38, 2001, p. 8503-8527.

Chambon R., Crochepeyre S., Charlier R., “An algorithm and a method to search bifurcation points in non-linear problems”, International Journal for Numerical Methods in Engineering, vol. 51, 2001, p. 315–332.

Charlier R., Collin F., Pardoen B., Talandier J., Radu JP., Gerard P., “An unsaturated hydro-mechanical modelling of two in-situ experiments in callovo-oxfordian argillite”. Engineering Geology, 2012, submitted.

Collin F., Chambon R., Charlier R., “ A finite element method for poro mechanical modelling of geotechnical problems using local second gradient models”, International Journal for Numerical Methods in Engineering, vol. 65, n° 11, 2006, p. 1749–1772.

Cruchaudet M., Noiret A., Talandier J., Armand G., “Expérimentation SDZ – Bilan de la mise en place de l’instrumentation et des premières mesures à fin mars 2010 – Centre de Meuse/Haute-Marne”, rapport interne n° D.RP.AMFS.09.0087, 2010a, ANDRA.

Cruchaudet M., Noiret A., Talandier J., Gatmiri B., Armand G., “OHZ en GED : EDZ initiale et évolution”, rapport interne n° D.RP.AMFS.11.0016, 2010b, ANDRA.

Germain P., “The method of virtual power in continuum mechanics. Part 2 Microstructure”, SIAM Journal on Applied Mathematics, vol. 25, 1973, p. 556-575.

Mindlin R.D., “Micro-structure in linear elasticity”, Archive for Rational Mechanics and Analysis, vol. 16, 1964, p. 51–78.

Sieffert Y., Al Holo S., Chambon R., "Loss of uniqueness of numerical solutions of the borehole problem modelled with enhanced media", International Journal of Solids and Structures, vol. 46, 2009, p. 3173–3197.

Toupin R., “Elastic materials with couple–stresses”, Archive for Rational Mechanics and Analysis, vol. 11, 1962, p. 385–414.

Zervos A., Papanastasiou P., Vardoulakis I., “Modelling of localisation and scale effect in thick-walled cylinders with gradient elastoplasticity”, International Journal of Solids and Structures, vol. 38, 2001, p. 5081-5095.